energies

MDPI

Article

Investigation and Validation of Unstructured Mesh Methodologies for Modeling Experimental Reactors

Tom Mager [1,*], Carlo Fiorina [1], Mathieu Hursin [2] and Andreas Pautz [1,2]

[1] École Polytechnique Fédérale de Lausanne, Laboratory for Reactor Physics and Systems Behaviour, 1015 Lausanne, Switzerland; carlo.fiorina@epfl.ch (C.F.); andreas.pautz@epfl.ch (A.P.)
[2] Paul Scherrer Institut, Laboratory for Reactor Physics and Systems Behaviour, Nuclear Energy and Safety Department, PSI, 5132 Villigen, Switzerland; mathieu.hursin@epfl.ch
* Correspondence: tom.mager@epfl.ch

Abstract: This paper summarizes a methodology developed at École Polytechnique Fédérale de Lausanne for the neutronic modeling of the CROCUS experimental reactor and proposes solutions to the challenges one may face while modeling a research reactor with a complex geometry. Indeed, the double-lattice configuration of CROCUS makes it difficult to use codes for neutron diffusion and transport relying on a structured mesh description. For this reason, and based on the available in-house competences, we decided to make use of the neutronic capabilities of the GeN-Foam multiphysics solver, which takes advantage of general finite volume methodologies on unstructured meshes to provide sufficient flexibility for the study of unconventional reactor designs. In this work, GeN-Foam is used to build a first SP_3 model of CROCUS based on an unstructured mesh to have an explicit modeling of the double lattice and the water gap between the two lattices. Form functions are then used to reconstruct the intra-pin fission rates for validation against measured distributions. We also discuss the limitations of the SP_3 approximation of neutron transport in regions with steep neutron flux gradients and the planned future developments.

Keywords: GeN-Foam; unstructured mesh; SP3; neutron transport; CROCUS

Citation: Mager, T.; Fiorina, C.; Hursin, M.; Pautz, A. Investigation and Validation of Unstructured Mesh Methodologies for Modeling Experimental Reactors. *Energies* **2022**, *15*, 1512. https://doi.org/10.3390/en15041512

Academic Editor: Dan Kotlyar

Received: 20 January 2022
Accepted: 16 February 2022
Published: 18 February 2022

1. Introduction

Several computational tools have been developed over the last 50 years for the full-core 3D analysis of power nuclear reactors. However, the use of these tools for modeling experimental reactors is not always possible as their geometry and operating features largely differ from one design to another. The CROCUS experimental reactor [1] operated on the École Polytechnique Fédérale de Lausanne campus is one of the research reactors whose heterogeneities are difficult to model accurately by nodal diffusion codes such as PARCS [2] or by recent high fidelity full core neutron solvers such as MPACT [3] or nTRACER [4]; as those codes rely on a structured mesh description of the geometry. As a result, the Monte Carlo particle transport code Serpent [5] remains the reference tool for CROCUS analysis. A previous attempt at modeling the core with PARCS is reported in [6], but the neutron flux comparison with the Serpent solution was not successful, especially in the outer fuel lattice region, due to the mismatch between PARCS mesh and the actual CROCUS fuel lattices. Furthermore, in line with the current efforts towards the use of more flexible numerical methodologies to implement deterministic neutron transport solvers capable of operating on unstructured meshes [7,8], the Laboratory for Reactor Physics and System Behaviour (LRS-EPFL) has started to develop new tools for reactor analysis based on the OpenFOAM finite-volume library [9,10], namely: the GeN-Foam multiphysics solver [11] and the OFFBEAT fuel behavior tool [12]. In particular, GeN-Foam is a multiphysics solver for the analysis of nuclear reactors that takes advantage of general finite-volume methodologies on unstructured meshes to provide enough flexibility

for the study of non-conventional reactor designs, such as CROCUS. Therefore, GeN-Foam offers an excellent opportunity to build an unstructured model of CROCUS with explicit modeling of the two fuel lattices and the water gap in-between them. The results of the GeN-Foam SP_3 solver obtained both with a structured and an unstructured mesh are compared in this paper to existing fission rates distribution and control rod reactivity worth measurements [13].

2. The CROCUS Experimental Reactor

CROCUS is a zero power reactor operated on the EPFL campus. With its maximum allowed power of 100 W, dose rates inside the shielding are acceptably low after shutdown. Thus, the reactor can be flexibly used for teaching and research. The core, schematized in Figure 1, is located in an aluminum vessel of 1.3 m diameter and 1.2 cm thickness. This vessel is the outer boundary holding the demineralized light water used both as moderator and reflector. The core active part has the approximate shape of a 60-cm diameter and 1-m high cylinder. It consists of two fuel zones with squares lattices of different pitches:

- an inner uranium oxide region with 336 rods enriched to 1.806% and a pitch of 1.837 cm;
- an outer uranium metal region with 176 rods enriched to 0.947% and a pitch of 2.917 cm.

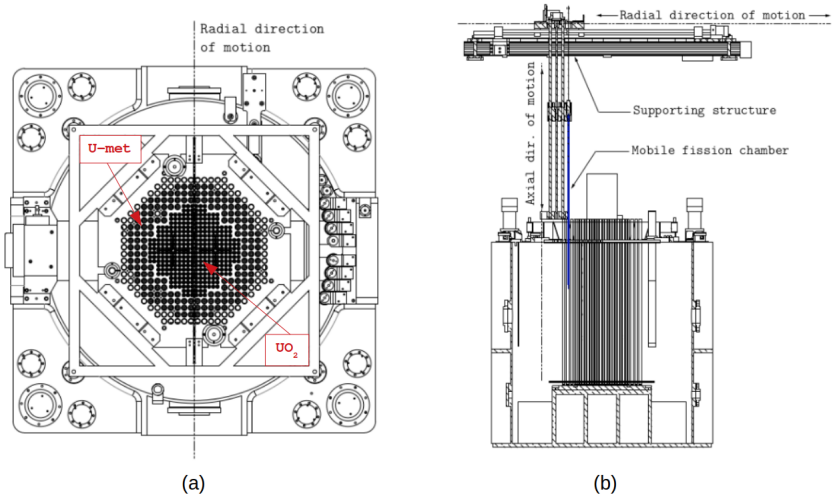

Figure 1. Schematics of CROCUS: (**a**) Top-view of the loading pattern with the inner UO_2 and outer U-metal lattices and (**b**) axial section of the reactor vessel and its internal structures. The Translateur Radial AXial (TRAX) system for in core fission chambers measurements [14] is displayed on both views.

Due to their different pitches, a water layer stands in between the two zones, which prevents the use of a structured mesh for matching every pin cell. The two uranium fuels consist of a stack of aluminum-coated cylindrical pellets. The fuel rods are held in position by two octagonal aluminum grids spaced one meter apart. A 0.5 mm layer of cadmium is placed in the mid-plane of each of these aluminum plates to limit the axial heat flux and neutron doses in the reactor cavity. The active fuel zone is therefore located between the two cadmium layers. The reactor can be controlled in two distinct ways, one using the B_4C control rods and the other using the water level in the vessel, the position of which can be finely adjusted by means of a spillway. With the current fuel loading, the critical water level is 952.2 $\pm$ 0.1 mm with both rods fully withdrawn. Therefore, as shown in Figure 1, a small axial section of the active core is exposed to air at atmospheric conditions.

3. Measurements Already Performed in CROCUS

The CROCUS zero power reactor offers privileged access to the fuel lattice for the realization of in-core measurements. During a previous project, radial and axial fission rate distributions in CROCUS were measured using a miniature fission chamber loaded

with ^{235}U (90 wt%-enriched) [15]. The position of the fission chamber was controlled by the TRAX system, displayed in Figure 1, which allows vertical and radial displacement of the chamber with 1 mm precision. The control rods' reactivity worth were also measured thanks to withdrawal and insertion experiments. Both these measurements are used for the validation of the unstructured GeN-Foam model of the CROCUS reactor.

4. The GeN-Foam Multiphysics Solver

Over the past few years, the Laboratory of Reactor Physics and System Behaviour at PSI and EPFL has developed a new code for reactor analysis, based on OpenFOAM, an open-source C++ library for solving partial differential equations using finite volume discretization. The resulting tool, called GeN-Foam, is a multiphysics solver for steady-state and transient nuclear reactor analysis [11]. It couples together a multiscale fine/coarse mesh subsolver for thermal hydraulics (one and two phases) [16,17], a subsolver for neutronics (point kinetics [18], diffusion [19], SP3 [20], and SN [21,22]), and a displacement-based subsolver for thermal-mechanics to allow deforming the neutronics mesh for an explicit modeling of the expansion reactivity feedback. The developed solver can easily be maintained and modified thanks to object-oriented programming. It also supports modern parallel computing, the use of general unstructured meshes, and mesh deformation capabilities. The parametrization of cross-sections can be performed cell by cell, and the energy group structure choice is completely arbitrary since the energy grid for homogenization is user defined. In particular, the capability to operate on an unstructured mesh and its parallel scalability make GeN-Foam a well-suited tool for the analysis of CROCUS.

5. GeN-Foam Modeling of CROCUS

In the GeN-Foam SP_3 model of CROCUS, two groups of cross-sections have been generated based on dedicated full core Serpent calculations [20], with the following homogenization regions: inner core, outer core, control rod, and reflector, as displayed in Figure 2. Each of these regions has been separated into a submerged and an emerged part. The lower and upper structures of the reactors were not considered in order to avoid the very sharp change in cross-sections occurring at their interface with the active core. A reduced geometry of the core was for this reason modeled, including only the structures placed axially in between the two cadmium layers, and proper albedo boundary conditions were set at the top and bottom boundaries. A gradual refinement of the mesh towards the cadmium layers was used in the axial direction, as shown in Figure 3c, allowing correct reproduction of the steep flux drop at boundaries.

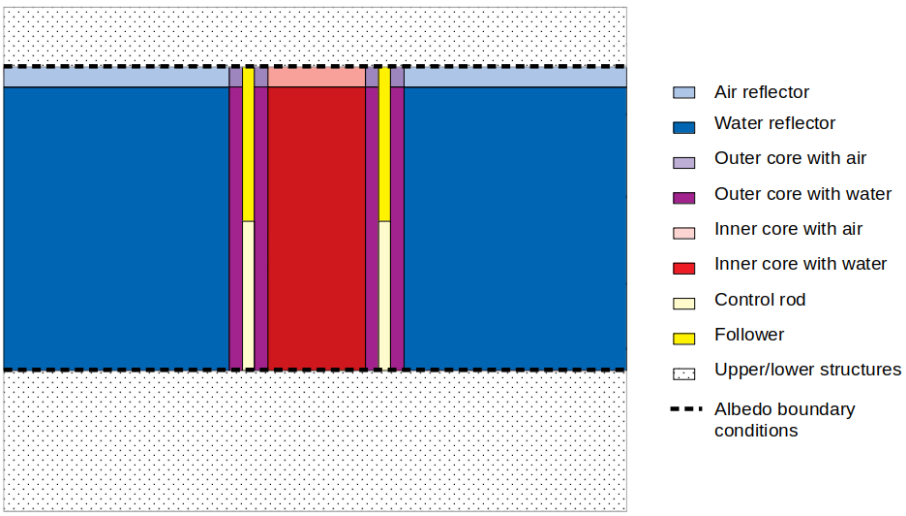

Figure 2. Geometry used for GeN-Foam calculations along with the name of the universes used in Serpent for cross-section homogenization.

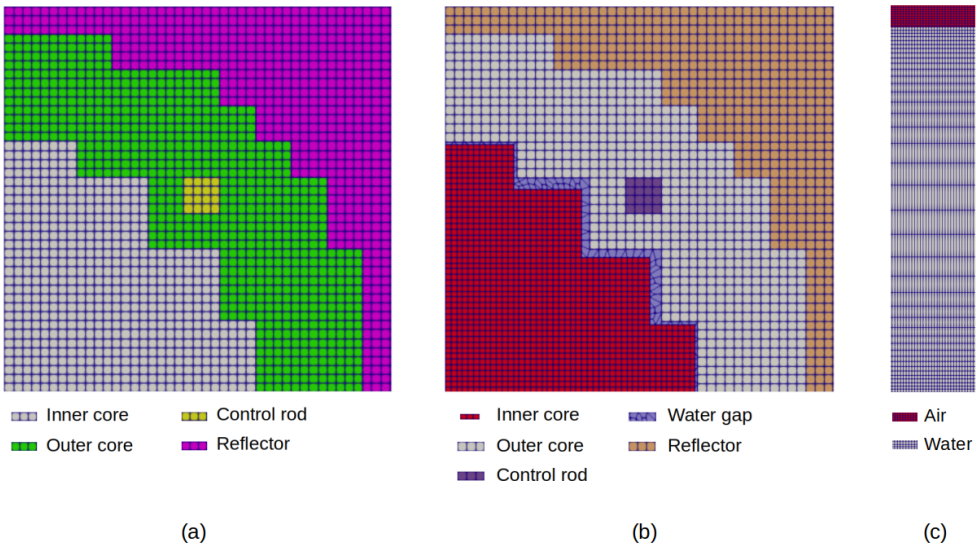

Figure 3. Top view of both the structured (**a**) and the unstructured (**b**) meshes with universe names. Only a reduced quarter of each is displayed to allow for a clear view of the boundaries between regions. The axial mesh refinement is also presented in panel (**c**).

Regarding the radial discretization, two different models have been implemented and compared:

- a "structured model", with a single regular mesh based on the outer core lattice, presented in Section 5.1;
- an "unstructured model", with two regular meshes based on the inner and outer core lattices, and a third one for the water gap linking the two, presented in Section 5.2;

The reduced geometry of CROCUS from Figure 2 was directly built in the mesh generator Salome [23]. The meshing algorithms used will be described in Sections 5.1 and 5.2. The resulting meshes were exported to the UNV mesh format, which can be translated into the foam format thanks to a dedicated OpenFoam mesh conversion routine [24].

5.1. GeN-Foam Structured Model

Since CROCUS consists of two fuel zones with square lattices of different pitches, we had to choose which base grid to use for the structured mesh. If the mesh was based on the inner core pitch, the boundary between the outer core and the reflector region would not have matched the mesh cells. Therefore, we chose here the outer core pitch, which consists of a U-met pin, as a base grid. The resulting regular mesh was produced thanks to the quadrangle meshing algorithm from Salome. The water gap interface between the inner and outer core regions was thus homogenized with the inner core one. A 16 cells per pin radial discretization was used to obtain mesh convergence. The resulting mesh is displayed in Figure 3a. The structured mesh resulted in approximately six million cells with a radial cell length of $\sim$0.5 mm and an axial length of $\sim$1 mm in the proximity of the cadmium layers.

5.2. GeN-Foam Unstructured Model

Two groups of cross-sections were generated following the same method as for the structured model, with the difference that the water gap region is no longer part of the inner core region but stands as an independent Serpent universe leading to the generation of a dedicated set of homogenized cross-sections. A 16 cells per pin radial discretization was also used in both the inner and outer core regions to obtain mesh convergence, and the NETGEN algorithm [25] with quadrangles preference from Salome was used in the water gap region linking the two regular fuel lattices, as displayed in Figure 3b. One may notice a relatively low quality mesh in the water gap, as we could not find algorithms in Salome

that allowed us to obtain better quality meshes in that region in a straightforward manner. Fortunately, as discussed later, this seems to have a limited impact on results, aside from when attempting to use a very specific algorithm to connect the various regions. In the axial direction, the same discretization as for the structured model was used, resulting in a mesh of approximately eight million cells.

Two meshing solutions have been investigated for the inter-lattice water gap modeling. Either a mesh is created that links inner and outer core nodes, or a stand-alone mesh is implemented that results in non coincident nodes between both core regions. In the second option, the Arbitrary Mesh Interface coupling condition (cyclic AMI) from OpenFOAM [26] can be used to pass information from one mesh to the other. A 253 pcm difference in k_{eff} was observed between the two solutions and the calculation with AMI coupling conditions took about 15% longer. Refining the mesh axially or radially did not reduce the difference.

A 2D test case was then used to understand the causes for the discrepancy. The test case consists of a 2D square with a fuel region at the bottom left corner and a reflector region elsewhere. Three different meshing solutions were implemented and are displayed in Figure 4a: a reference one with a regular mesh all over the space; a solution with AMI coupling condition at the boundary between the fuel and reflector regions; and another solution without AMI. Thermal neutron flux traverses along the white arrow have been plotted for the three cases in Figure 4b, along with a zoom at the fuel—reflector interface. The relative error for the reference solution has also been plotted in the panel (c) to better visualize the difference between the "with AMI" and "without AMI" cases. A +8% relative error in the thermal flux compared to the reference can be seen with AMI, while it drops to only +1% without it; this could partly explain the +253 pcm difference observed for the two whole core cases. Both solutions also seem to underestimate the flux in cells immediately before the interface, −5% with AMI and −6% without, whose impact on the k_{eff} difference observed is less evident. In general, we suspect that the numerical reason for the inaccuracy introduced by the AMI treatment could be associated with the fact that the AMI methodology imposes the continuity of fields (the fluxes, in this case) at a certain boundary, while not necessarily guaranteeing the conservation of currents, and thus neutron balances. This may play a particularly significant role in the case of non-orthogonal or skewed meshes such as those that we have in the water gap of the full-core model. The unstructured mesh of Figure 3b is, therefore, for the time being the chosen solution for our GeN-Foam model of CROCUS, while further investigation into the use of AMI is deferred to future studies. In particular, we plan in the future to investigate the possibility to obtain a regular mesh in the water gap, which should minimize the interpolation errors introduced by the AMI.

5.3. Comparison of GeN-Foam Models

Eigenvalue calculations with the SP3 solver were performed for both the structured and the unstructured models. The resulting k_{eff} are summarized in Table 1, along with a Monte Carlo reference obtained with Serpent 2.1.31. The neutron population for the serpent calculation was set at 10^6 neutrons per generation, with 200 inactive and 5000 active generations. The nuclear data library used was ENDF/B-VII.0, along with the Serpent transport correction (trc) for the calculation of transport cross-section and diffusion coefficient. A transport correction ratio [27] was multiplied to material total cross sections to obtain transport cross sections. The unstructured model presents a k_{eff}, which is 83 pcm closer to the Serpent2 reference.

Table 1. Comparison between Serpent and both GeN-Foam models results in terms of k_{eff}.

		k_{eff} **(Value)**	**dk/k w. Serpent (pcm)**
Serpent 2 (trc)		0.999543 ±1 pcm	-
GeN-Foam SP3	structured mesh	0.995187	−435
	unstructured mesh	0.996024	−352

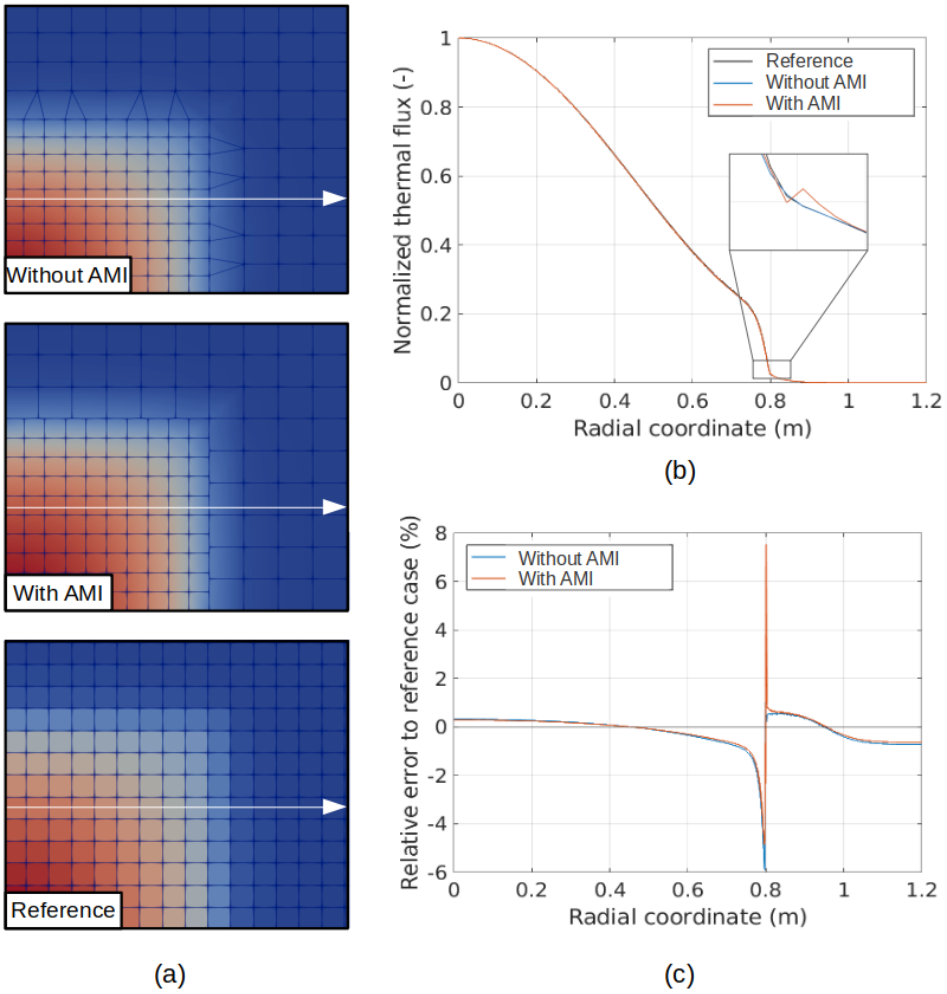

Figure 4. Arbitrary Mesh Interface (AMI) coupling condition study: (**a**) meshes used for the three test cases, (**b**) thermal neutron flux traverses, and (**c**) their relative error to the reference case.

The main difference between the structured and the unstructured model lies in the modeling of the water gap. As a result, the neutron flux deflections will be mainly observed in the thermal domain. Therefore, only the axial and radial profiles of the thermal neutron flux are shown in Figure 5, in order to compare the two models in more detail.

One can first notice in Figure 5a,b that the thermal neutron flux is higher in the inner core region for the structured model than for the unstructured one, even though the structured k_{eff} is lower than the unstructured. This is due to the inter-lattice water gap that is spread out in the inner core region for a model with a structured mesh. Therefore, in the process of generating the cross-sections, the cross-section of the inner core region has been homogenized by taking into account this extra slice of water, whose effect on neutron thermalization is quite large: $\sim 0.5 \cdot 10^{12}$ m$^{-2}\cdot$ s^{-1} difference at the core center. This effect is counterbalanced in the unstructured model by an increase in the thermal flux near the water gap, which can be seen in Figure 5b. This increase may seem negligible compared to the difference in neutron flux between the two models in the core center, but it should be kept in mind that this radial profile is a 1D representation of a 3D cylindrical geometry. Indeed, if we have a look at the three axial traverses in Figure 5c–e, the closer the rod is to the water gap, the larger the thermal flux difference between both GeN-Foam models. In rod (c), the difference between structured and unstructured models is even larger than the one observed at the core center. Then, the observed difference diminishes in rod (d), which has only one side directly in contact with the water gap, and completely vanishes in rod (e), which is in the middle of the outer fuel lattice.

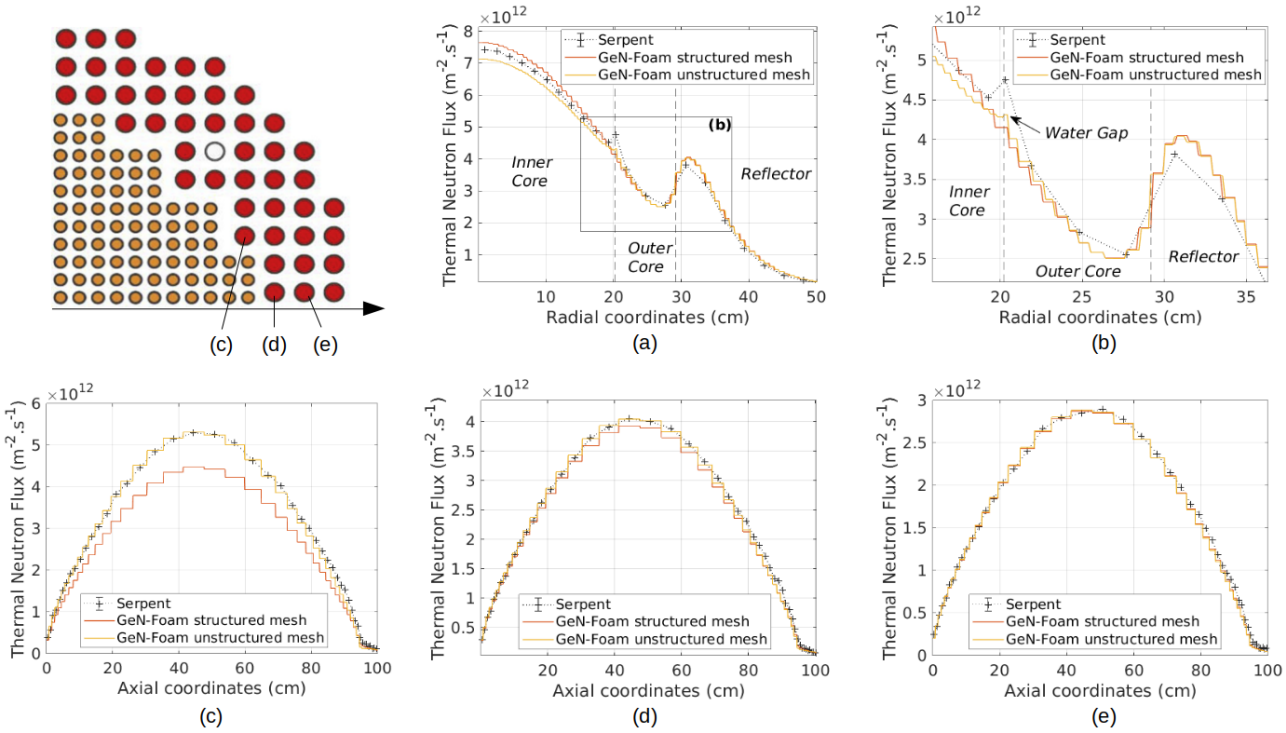

Figure 5. Comparison of both GeN-Foam models through thermal neutron flux profiles: (**a**) radial traverse from core center to the vessel (along the arrow on the upper-left scheme of CROCUS' loading pattern) with (**b**) a zoom on the outer core region, and (**c**–**e**) axial traverses in three different outer core fuel rods. Serpent 2 predictions for each pin cell are also displayed as a reference.

6. GeN-Foam Unstructured Model Validation

Fission rates and control rod reactivity worth measurements already performed at the CROCUS reactor [15], and described in Section 3, were used to validate the GeN-Foam model.

6.1. Fission Rates

Although GeN-Foam is able to model neutron flux profiles, as shown in Figure 5, they only provide cell-wise information. Form functions are required to reconstruct within-cell heterogeneities (e.g., the response of a detector inserted there) from the homogeneous solution. Form functions (FF) are defined as

$$R_f^{het}(\mathbf{r}) = R_f^{hom}(\mathbf{r}) \cdot FF(\mathbf{r}) \tag{1}$$

where R_f stands for the fission rate.

Serpent was employed to compute these form functions. While the homogeneous fission rate (R_f^{hom}) distribution was directly obtained from GeN-Foam, the heterogeneous fission rate (R_f^{het}) was computed thanks to dedicated Serpent pin-cell calculations, one for each fuel rod type. To tally this heterogeneous fission rate with Serpent, a pin-cell was subdivided into 16 smaller volumes, and R_f^{het} was approximated as the average fission rate in each of these volumes.

The form functions were then computed as

$$FF(i) = \frac{R_f^{het}(i)}{\sum_{k=1}^{16} R_f^{het}(k)} \tag{2}$$

where i represents the indices for the Serpent detector volumes.

Thanks to these form functions, fission rate profiles can be obtained with GeN-Foam and compared to Serpent fission rates and to the TRAX fission chamber measurements. While the pin-by-pin power reconstruction was performed on the whole radial traverse for the GeN-Foam unstructured model, it was only made in the outer core region for the structured model, since it is the only region where fuel pins are matching the structured mesh. The full results are shown in Figure 6. All fission rates are normalized to their maximum value at the core center.

On the zoom into the outer core region in Figure 6a, the unstructured GeN-Foam model appears to better match the Serpent reference solution. This is clearly represented in Figure 6b, where the two models, structured and unstructured, are compared to the Serpent solution. Error bars due to Serpent stochastic predictions appear directly on the C/E ratios, which explain the erratic changes observed from one mesh cell to the other. While both models show similar trends near the reflector, the unstructured mesh clearly helps in modeling the water gap and its near vicinity. For validation purposes, the GeN-Foam fission rate profiles obtained with both models were compared to the ^{235}U fission chamber measurements, as shown in Figure 6c. The unstructured mesh models the outer region of the core better, as demonstrated by a smaller RMS difference (see the upper right corner of the figure).

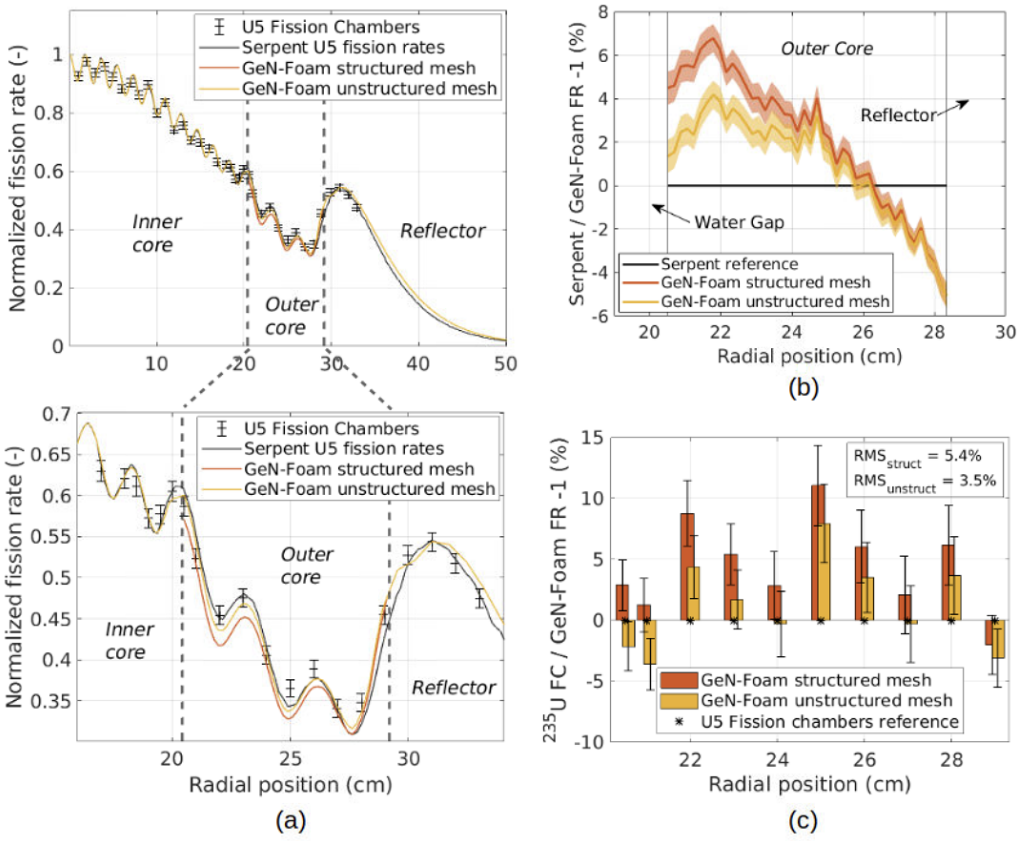

Figure 6. (**a**) Fission rate radial profiles, normalized to their core center values. Pin-by-pin power reconstruction was performed on the GeN-Foam profiles. (**b**) Code to code and (**c**) code to experiments validation of the GeN-Foam model, with a focus on the outer core region.

6.2. Control Rod Reactivity Worth

Table 2 summarizes the experimental control rods' reactivity worth as well as those computed with Serpent and GeN-Foam for both the structured and the unstructured mesh. While the experimental values and Serpent's predictions are in agreement, the SP_3 solver of GeN-Foam presents statistically significant differences with Serpent's results. A notable difference can be observed between the structured and unstructured mesh results, but drawing conclusions only based on these SP_3 solver results would be premature

as the k_{eff} quantity is error cancellation prone. Indeed, the SP_3 solver is not suited for the analysis of local effect where steep flux gradients take place, especially in the vicinity of the control rod. A neutron transport solver, based for instance on the discrete ordinates methodology, would provide better results.

Table 2. Experimental control rod reactivity worth compared to Serpent and GeN-Foam.

	Reactivity Worth (pcm)
Experimental (JEFF-3.1.1 & U235 JEF/DOC-920) Retrieved from [15].	
SE control rod - withdrawal NW control rod - withdrawal	175.8 ± 6.0 178.7 ± 6.0
Serpent 2	
SE control rod NW control rod	172.0 ± 1.3 172.0 ± 1.3
GeN-Foam SP_3 (Reduced geometry with structured mesh)	
SE control rod NW control rod	179.5 179.5
GeN-Foam SP_3 (Reduced geometry with unstructured mesh)	
SE control rod NW control rod	167.0 167.0

6.3. Computational Costs

The capacity of OpenFOAM to operate on unstructured meshes comes with the drawback of a large memory footprint and computational requirements [10]. Large amounts of memory are required to store nodes, faces, volumes, connectivity and fields, which in turn affects the computation time by the communication of this information between the processor and RAM. More importantly, the use of unstructured meshes makes it difficult to implement optimized methods, such as iterative 1-D sweepings, that make use of prior knowledge about the shape of cells. The lack of prior knowledge about the mesh makes it also more difficult to develop specialized accelerators (such as multigrid accelerators). On the other hand, it is worth mentioning that OpenFOAM scales linearly up to several thousand cores [28], which can significantly speed up computational times when modern computational resources are available.

7. Discussion

A SP_3 GeN-Foam model of the CROCUS experimental reactor, taking advantage of the OpenFOAM unstructured mesh features, has been compared with existing measurements of fission rate distributions and control rod reactivity worth. Simulations were carried out using two groups of cross-sections generated by a dedicated full core Serpent calculation. Form functions successfully allowed reconstruction of the fission rate variations within the GeN-Foam mesh. The use of an unstructured mesh appears to be a solution for an accurate modeling of the flux distribution in the two different lattices of CROCUS and of the resulting water gap. However, this SP_3 GeN-Foam model fails to accurately reproduce measured control rod reactivity worth, pointing out the limitations of the SP_3 approximation to neutron transport in regions with steep neutron flux gradients, notably when discontinuity factors are not used. The next step would therefore be the use of the discrete ordinate solver of GeN-Foam [22] along with a heterogeneous geometry description, to move towards a high fidelity modeling of CROCUS with pin-resolved neutron transport calculations.

Author Contributions: Conceptualization, T.M. and M.H.; methodology, T.M., M.H. and C.F.; software, T.M. and C.F.; validation, M.H. and C.F.; formal analysis, T.M.; investigation, T.M., M.H. and C.F.; resources, A.P.; data curation, T.M. and C.F.; writing—original draft preparation, T.M.; writing—review and editing, T.M., M.H. and C.F.; visualization, T.M.; supervision, M.H. and C.F.; project administration, A.P.; funding acquisition, A.P. All authors have read and agreed to the published version of the manuscript.

Funding: This research received no external funding.

Institutional Review Board Statement: Not applicable.

Informed Consent Statement: Not applicable.

Conflicts of Interest: The authors declare no conflicts of interest.

References

1. CROCUS Experimental Reactor. Available online: https://www.epfl.ch/labs/lrs/facilities/crocus-reactor/ (accessed on 14 January 2022).
2. Downar, T.; Barber, D.; Miller, R.M.; Lee, C.; Kozlowski, T.; Lee, D.; Xu, Y.; Gan, J.; Joo, H.; Cho, J.; et al. PARCS: Purdue advanced reactor core simulator. In Proceedings of the PHYSOR 2002—International Conference on the New Frontiers of Nuclear Technology: Reactor Physics, Safety and High-Performance Computing—The ANS 2002 RPD Topical Meeting, Seoul, Korea, 7–10 October 2002.
3. Kochunas, B.; Collins, B.; Jabaay, D.; Downar, T.J.; Martin, W.R. Overview of development and design of MPACT: Michigan parallel characteristics transport code. In Proceedings of the M&C 2013—International Conference on Mathematics & Computational Methods Applied to Nuclear Science & Engineering, Sun Valley, ID, USA, 5–9 May 2013.
4. Jung, Y.S.; Shim, C.B.; Lim, C.H.; Joo, H.G. Practical numerical reactor employing direct whole core neutron transport and subchannel thermal/hydraulic solvers. *Ann. Nucl. Energy* **2013**, *62*, 357–374. [CrossRef]
5. Leppänen, J.; Pusa, M.; Viitanen, T.; Valtavirta, V.; Kaltiaisenaho, T. The Serpent Monte Carlo code: Status, development and applications in 2013. *Ann. Nucl. Energy* **2015**, *82*, 142–150. [CrossRef]
6. Rais, A.; Siefman, D.; Hursin, M.; Ward, A.; Pautz, A. Neutronics modeling of the CROCUS reactor with SERPENT and PARCS codes. In Proceedings of the M&C 2017—International Conference on Mathematics & Computational Methods Applied to Nuclear Science & Engineering, Jeju, Korea, 16–20 April 2017.
7. Vermaak, J.I.; Ragusa, J.C.; Adams, M.L.; Morel, J.E. Massively parallel transport sweeps on meshes with cyclic dependencies. *J. Comput. Phys.* **2021**, *425*, 109892. [CrossRef]
8. Gaston, D.R.; Forget, B.; Smith, K.S.; Harbour, L.H.; Ridley, G.K.; Giudicelli, G.G. Method of Characteristics for 3D, Full-Core Neutron Transport on Unstructured Mesh. *Nucl. Technol.* **2021**, *207*, 931–953. [CrossRef]
9. OpenFoam. Available online: https://openfoam.com/ (accessed on 14 January 2022).
10. Fiorina, C.; Clifford, I.; Kelm, S.; Lorenzi, S. On the development of multi-physics tools for nuclear reactor analysis based on OpenFOAM®: State of the art, lessons learned and perspectives. *Nucl. Eng. Des.* **2021**, *387*, 111604. [CrossRef]
11. Fiorina, C.; Clifford, I.; Aufiero, M.; Mikityuk, K. GeN-Foam: A novel OpenFOAM based multi-physics solver for 2D/3D transient analysis of nuclear reactors. *Nucl. Eng. Des.* **2015**, *294*, 24–37. [CrossRef]
12. Scolaro, A.; Clifford, I.; Fiorina, C.; Pautz, A. The OFFBEAT multi-dimensional fuel behavior solver. *Nucl. Eng. Des.* **2020**, *358*. [CrossRef]
13. Rais, A.; Siefman, D.; Girardin, G.; Hursin, M.; Pautz, A. Methods and Models for the Coupled Neutronics and Thermal-Hydraulics Analysis of the CROCUS Reactor at EFPL. *Sci. Technol. Nucl. Install.* **2015**, *2015*, 237646. [CrossRef]
14. Rais, A. Performance Assessment of a 3-D Steady-State and Spatial Kinetics Model for the CROCUS Reactor. Ph.D. Thesis, EPFL, Lausanne, Switzerland, 2018.
15. Rais, A.; Hursin, M.; Perret, G.; Pautz, A. Experimental validation of control rod reactivity worth and fission rate distributions for the CROCUS Reactor. In *Physics of Reactors 2016 (PHYSOR 2016): Unifying Theory and Experiments in the 21st Century*; American Nuclear Society (ANS): Sun Valley, ID, USA, 2016.
16. Radman, S.; Fiorina, C.; Pautz, A. Development of a novel two-phase flow solver for nuclear reactor analysis: Validation against sodium boiling experiments. *Nucl. Eng. Des.* **2021**, *384*, 111422. [CrossRef]
17. Radman, S.; Fiorina, C.; Pautz, A. Development of a novel two-phase flow solver for nuclear reactor analysis: Algorithms, verification and implementation in OpenFOAM. *Nucl. Eng. Des.* **2021**, *379*, 111178. [CrossRef]
18. Radman, S.; Fiorina, C.; Song, P.; Pautz, A. Development of a point-kinetics model in OpenFOAM, integration in GeN-Foam, and validation against FFTF experimental data. *Ann. Nucl. Energy* **2021**, 168, 108891. [CrossRef]
19. Fiorina, C.; Kerkar, N.; Mikityuk, K.; Rubiolo, P.; Pautz, A. Development and verification of the neutron diffusion solver for the GeN-Foam multi-physics platform. *Ann. Nucl. Energy* **2016**, *96*, 212–222. [CrossRef]
20. Fiorina, C.; Hursin, M.; Pautz, A. Extension of the GeN-Foam neutronic solver to SP3 analysis and application to the CROCUS experimental reactor. *Ann. Nucl. Energy* **2017**, *101*, 419–428. [CrossRef]

21. Fiorina, C.; Radman, S.; Koc, M.Z.; Pautz, A. Detailed modelling of the expansion reactivity feedback in fast reactors using OpenFoam. In Proceedings of the International Conference on Mathematics and Computational Methods Applied to Nuclear Science and Engineering, M and C, Portland, OR, USA, 25–29 August 2019.
22. Fiorina, C.; Aufiero, M.; Pelloni, S.; Mikityuk, K. A time-dependent solver for coupled neutron-transport thermal-mechanics calculations and simulation of a godiva prompt-critical burst. In *International Conference on Nuclear Engineering, Proceedings, ICONE*; American Society of Mechanical Engineers: Florence, Italy, 2014. [CrossRef]
23. Salome Platform. Available online: https://www.salome-platform.org/ (accessed on 14 January 2022).
24. IdeasUnvToFoam Mesh Conversion Routine, Openfoam. Available online: https://www.openfoam.com/documentation/guides/latest/man/ideasUnvToFoam.html (accessed on 14 January 2022).
25. NETGEN Meshing Algorithm, Salome Platform. Available online: https://docs.salome-platform.org/latest/gui/NETGENPLUGIN/netgen.html (accessed on 14 January 2022).
26. AMI Boundary Condition, OpenFoam. Available online: https://www.openfoam.com/documentation/guides/latest/doc/guide-bcs-coupled-cyclic-ami.html (accessed on 14 January 2022).
27. Herman, B.; Forget, B.; Smith, K.; Aviles, B. Improved diffusion coefficients generated from Monte Carlo codes. In Proceedings of the International Conference on Mathematics and Computational Methods Applied to Nuclear Science and Engineering, Sun Valley, ID, USA, 16–20 April 2013.
28. Fiorina, C.; Amati, G.; Ruggiero, V.; Spisso, I. Partnership for Advanced Computing in Europe SHAPE Project Milano Multiphysics: Evaluation of the Intel Xeon Phi Performances for High Fidelity Nuclear Applications. Available online: https://prace-ri.eu/wp-content/uploads/WP267.pdf (accessed on 14 January 2022).